A novel method for the genome-wide high resolution analysis of DNA damage

Yumin Teng[1], Mark Bennett[1], Katie E. Evans[1], Huayun Zhuang-Jackson[1], Andy Higgs[2], Simon H. Reed[1] and Raymond Waters[1,*]

[1]Department of Medical Genetics, Haematology and Pathology, School of Medicine, Cancer Genetics Building, Cardiff University, Heath Park, Cardiff CF14 4XN and [2]Agilent Technologies UK Limited, Winnersh Triangle, Wokingham, Berkshire RG41 5TP, UK

ABSTRACT

DNA damage occurs via endogenous and exogenous genotoxic agents and compromises a genome's integrity. Knowing where damage occurs within a genome is crucial to understanding the repair mechanisms which protect this integrity. This paper describes a new development based on microarray technology which uses ultraviolet light induced DNA damage as a paradigm to determine the position and frequency of DNA damage and its subsequent repair throughout the entire yeast genome.

INTRODUCTION

DNA damage occurs via endogenous and exogenous genotoxic agents, generating base losses and modifications, strand breaks, crosslinks, bulky chemical adducts and other DNA alterations (1). If this damage remains unrepaired, it will impact on DNA metabolism, result in abnormal cellular activity and it can cause mutation or cell death. To maintain genome integrity, cells have evolved a variety of DNA repair mechanisms. One of these is nucleotide excision repair (NER) which is well conserved during evolution. In humans a NER deficiency predisposes affected individuals to a cancer-prone genetic disorder, xeroderma pigmentosum (1).

NER removes a wide range of DNA lesions, and often recognizes damages that distort the DNA helical structure including ultraviolet light (UV) induced cyclobutane pyrimidine dimers (CPDs). More than 30 repair proteins have been identified as having roles in NER on naked DNA templates *in vitro* (1). In cells, DNA is tightly packaged as chromatin and this poses a barrier to the operation of these core proteins. The roles of these core proteins were identified in part via studies with *Saccharomyces cerevisiae*, and where NER has many homologous steps to the mechanism in humans (1). How NER operates in the context of chromatin remains elusive although some inroads have been made in this area (2,3) often by employing methods to examine DNA damage and repair in specific regions of a genome.

Technologies are available to examine DNA damage and repair in selected genes (4) and certain damages can be analyzed at nucleotide resolution in some of those genes (5–7). However, none of these approaches are designed to examine repair events throughout genomes at a high resolution in order to identify the variations in repair rate and reveal any correlation of this with changes in chromatin structure. Such an approach would enable one to examine the global influence of factors on repair: for example, the accessibility of repair proteins to DNA damage in chromatin and the chromatin modification factors that facilitate its repair.

To address this, there was a need to develop a new approach to rapidly screen entire genomes for DNA damage and to measure their repair. DNA microarrays were developed decades ago for whole genome transcription profiling. The combination of these and chromatin immunoprecipitation, namely ChIP on chip, was an extension that enabled the identification of the binding sites of DNA-binding proteins and the covalent modifications to nucleosomes on a genome-wide basis (8,9). Here, we describe a genome wide approach that employs microarrays to monitor UV-induced DNA damage (CPDs) and its repair. Consequently, this enables us to identify the UV-induced changes in chromatin and the chromatin modifications that facilitate repair throughout an entire genome.

MATERIALS AND METHODS

UV irradiation

Yeast cells were collected from an overnight culture in Yeast Complete Medium (YPD) at a density of 2×10^7 cells/ml. Pre-chilled PBS (137 mM NaCl, 2.7 mM

---

*To whom correspondence should be addressed. Tel: +44 29 20687336; Fax: +44 29 20687343; Email: watersr1@cardiff.ac.uk

KCl, 4.3 mM Na_2HPO_4, 1.47 mM KH_2PO_4) was used to resuspend the cells at a density of 2×10^7 cells/ml. A fraction of cells (200 ml at 2×10^7 cells/ml) was kept on ice for the non-irradiated control sample (U). The number of cells for each sample was always the same and a non-irradiated control sample was always taken for each strain in every experiment. A batch of 50 ml of cell suspension was placed in a Pyrex dish ($\Phi = 14$ cm) and irradiated with 254 nm UV light at a dose of 50 J/m^2. The irradiated cells were kept in the dark in a sterile flask on ice. This irradiation step was repeated for the rest of the cell suspension. The same volume of UV treated cells taken for the U sample was collected to serve as a 0 sample with no repair time. The remainder of the UV-treated cells was collected by centrifugation and re-suspended in a flask of fresh YPD at 2×10^7 cells/ml and incubated at 30°C in the dark with vigorous shaking for subsequent DNA repair analysis. At the 2-h repair time point the same number of cells as for the U sample was taken from the repairing culture.

DNA preparation

Cells collected at each point were resuspended in 5 ml of sorbitol solution [0.9 M sorbitol, 0.1 M Tris–HCl (pH 8.0), 0.1 M EDTA]. 0.5 ml of zymolyase 20T (10 mg/ml in sorbitol solution, ICN Biochemicals, Inc.) and 0.5 ml of 0.28 M β-mercaptoethanol was added to each sample and mixed well by shaking. Cells were incubated at 30°C for 1 h in a shaking incubator. Spheroplasts were gently centrifuged at 3000 rpm for 5 min and resuspended in 5 ml of lysis buffer [4 M Urea, 200 mM NaCl, 100 mM Tris–HCl (pH 8.0), 10 mM CDTA, 0.5%(w/v) N-Lauroyl Sarcosine]/ PBS 1:1(v/v) solution. 0.5 ml of DNase-free RNase A at 3 mg/ml in TE buffer (Sigma-Aldrich, from bovine pancreas, prepared as a 10 mg/ml stock solution in 10 mM sodium acetate buffer pH 5.2, and boiled for 15 min at 100°C) was added to each sample. The samples were vortexed and incubated at 37°C for 1 h. Following this 0.5 ml of proteinase K (5 mg/ml in TE buffer, freshly made, Amresco) solution was added. The samples were incubated at 37°C for 1 h and then at 65°C for 1 h with occasional shaking. Phenol/chloroform (6 ml) and chloroform (6 ml) extractions were carried out prior to DNA precipitation with two volumes (12 ml) of pre-chilled 100% ethanol. DNA pellets were collected by centrifugation and resuspended in 1 ml of TE buffer. After being completely dissolved, the DNA samples were checked by non-denaturing agarose gel electrophoresis and UV spectrophotometry (ND-1000, NanoDrop Technologies Thermo scientific).

Fragmenting DNA by sonication

A bioruptor sonicator (Diagenode) was used to fragment DNA with the water temperature in the sonication tank kept at 4°C by a water circulation system. 1.5 ml Eppendorf tubes containing 300 μl of DNA samples in TE buffer were placed in a 1.5 ml microtube unit. Power was set to the 'High' position. Sonication was carried out for 20 s on and 40 s off for 12 cycles. Fragmented DNA was analyzed via agarose gel electrophoresis, and the

average fragment size was 400 bp (data not shown and http://www.diagenode.com/media/documents/downloads/ posters/PO-BR-A3-V2_22_06_10.pdf).

Immunoprecipitation (IP)

An amount of 50 μl of Dynabeads (Mouse lgG, Invitrogen) per sample were washed three times with 500 μl PBS-BSA (0.1%) per sample. The washed Dynabeads were resuspended in 100 μl of PBS-BSA (0.1%) per sample with the addition of the CPD antibody (Kamiya Biomedical Company, Seattle Anti-Thymine Dimer Clone KTM53 50 μl Dynabeads with 2–3 μl of the provided CPD antibody). The mixture was incubated at 30°C for 30 min at 1300 rpm in an Eppendorf Thermomixer. Dynabeads were collected and washed three times with 500 μl of PBS–BSA (0.1%), 4°C, and resuspended in 50 μl PBS-BSA (0.1%)/sample. The suspension was separated into 50-μl aliquots in fresh tubes and the supernatant removed. An amount of 100 μl of sonicated DNA samples were added to each tube containing the Dynabeads. An amount of 50 μl of 10× PBS–BSA (10 mg/ml) was added to each sample, and the final volume was adjusted to 500 μl with PBS. Samples were incubated at 21°C for 2 h at 1300 rpm in an Eppendorf Thermomixer followed by a wash with 500 μl of freshly prepared FA/SDS buffer (50 mM HEPES KOH pH 7.5, 150 mM NaCl, 1 mM EDTA, 1% Triton X-100, 0.1% Deoxycholate Na, 0.1% SDS, 1 mM PMSF). Further washes were as follows: three times wash with 1 ml of FA/SDS + NaCl (adjust the NaCl concentration to 500 mM); one wash with 500 μl of Li solution (100 mM Tris–Cl pH 9.0, 500 mM LiCl, 1% NP40, 1% deoxycholic Na), one wash with 500 μl of cold TE. DNA was eluted off the Dynabeads with 100 μl of Pronase (Promega) buffer (25 mM Tris pH 7.5, 5 mM EDTA, 0.5% SDS) at 65°C at 900 rpm for 20 min. An amount of 6.25 μl of Pronase (20 mg/ml, in H_2O) was added to each sample and incubated at 37°C for 1 h, then at 65°C in a water bath, overnight. The volume of the input samples (20 μl), was adjusted with TE buffer to 100 μl followed by the addition of 25 μl of 5× Pronase buffer (125 mM Tris pH 7.5, 25 mM EDTA, 2.5% SDS, 6.25 μl of Pronase at 20 mg/ml). They were then incubated as the IP samples. An amount of 1 μl of the DNase-free RNase A at 10 mg/ml was added to the IP and input samples followed by incubation at 37°C for 1 h. DNA was purified using the Qiagen PCR purification kit and eluted with 50 μl elution buffer.

Repair of DNA damages prior to PCR amplification

Immunoprecipitated DNA fragments obtained using the CPD antibody will contain CPD damage which will block DNA synthesis during the following PCR amplification step. Therefore, any damage has to be removed prior to PCR. The PreCR DNA repair kit (New England Biolabs) removes many DNA damages including CPDs. An amount of 40 μl of the IP samples and 1 μl of input samples diluted into 40 μl with H_2O, were subjected to repair treatment using the PreCR DNA repair kit as per

instructions. DNA was purify via a Qiagen PCR kit and eluted in 50 μl of elution buffer.

DNA end blunting and linker ligation

These were undertaken as described in the Agilent ChIP on chip protocol for Yeast (http://www.chem.agilent.com/ Library/usermanuals/Public/ChIP-on-chip_Yeast_ 9.2.pdf). In brief, 70 μl of a mixture of T4 DNA Pol Buffer (11 μl, NEB buffer 2 included with the T4 polymerase)., BSA (10 mg/ml, 0.5 μl), dNTP (10 mM, 1.0 μl), T4 DNA polymerase (0.2 μl from New England Biolabs (NEB). Catalog # MO203S), H_2O (57.8 μl) were added to 50 μl of IP sample or input sample on ice. The samples were mixed by pipetting and then incubated at 12°C in a water bath for 20 min. An amount of 11.5 μl of NaAc (3 M, pH5.2) and 0.5 μl of Glycogen (20 mg/ml) were added into each sample. After phenol/chloroform extraction, the DNA was precipitated with absolute ethanol (–80°C for 10 min). DNA was pelleted by centrifugation and washed once with cold 75% ethanol and resuspended in 25 μl of H_2O. An amount of 25 μl of ligation mix (13 μl of H_2O, 5 μl of DNA ligase buffer, 6.7 μl of linker hybrid, 0.5 μl of T4 DNA ligase) was added into each tube and mixed for overnight ligation at 16°C in a water bath. An amount of 6 μl of NaAc (3 M) was added to the ligation mixture and the DNA was precipitated with absolute ethanol at −80°C for 10 min. DNA was pelleted by centrifugation, washed once with cold 75% ethanol and resuspended in 25 μl of H_2O.

PCR amplification

Two steps of PCR were carried out as described in the Agilent ChIP on chip protocol with modifications. We did this so as we could archive reasonable amounts of each sample after the first PCR and re-analyze samples if required. For the first PCR, 15 μl of PCR mix (8 μl of 5× Buffer, 1.25 μl of 10 mM dNTP, 1.25 μl of 40 μM Oligo 102, 4.5 μl of H_2O) was added to each sample, and incubated at 55°C for 4 min in a PCR block. After the first 2-min incubation, the program was paused. An amount of 10 μl of Phusion DNA polymerase mixture (1 μl of Phusion Polymerase (New England Biolabs), 2 μl of 5× Buffer, 7 μl of H_2O) were added to each tube while the tube was kept in the heating block. The program was resumed and followed by 3 min incubation at 72°C. After a 1 min 98°C denaturing step, 25 cycles of PCR were applied as 10 s at 98°C, 30 s at 55°C and 1 min at 72°C, and the final step was 5 min at 72°C. Ten times dilution was made to each PCR by adding 450 μl of H_2O. This can be stored frozen for future use. A second PCR reaction with 5 μl of first PCR dilution and 45 μl of PCR mix (10 μl of 5× Buffer, 1.25 μl of 10 mM dNTP, 1.25 μl of 40 μM Oligo 102, 0.5 μl of Phusion DNA Pol, 32 μl of H_2O) was carried out using conditions of 98°C 1 min, 25 cycles of (98°C 10 s, 55°C 30 s, 72°C 1 min), 72°C 5 min. DNA was precipitated with the addition of 25 μl of 7.5 M Ammonium Acetate and 225 μl of absolute ethanol at −80°C for 10 min. DNA was pelleted by centrifugation and washed once with cold 75% ethanol and resuspended in 20 μl of H_2O. The concentration of DNA was measured with the NanoDrop spectrophotometer and all samples normalized to100 ng/μl with H_2O.

Labeling

The BioPrime Total Genomic Labeling System (Invitrogen) was used to label the DNA for ChIP on chip. Generally the IP samples were labeled with Alexa Fluor 5 (cy5) and the Input samples were labeled with Alexa Fluor 3 (cy3). An amount of 17.6 μl of amplified DNA samples (100 ng/μl) and 4.4 μl of 5 mM EDTA were placed in a 0.5 ml PCR tube. An amount of 25 μl of 2× Alexa Fluor 5 Reaction Mix or 2× Alexa Fluor 3 Reaction Mix were added into the tube and mixed. The samples were incubated at 95°C in the dark for 5 min and immediately cooled on ice for 5 min. While on ice, 3 μl of Exo-Klenow Fragment (40 units/μl and part of the BioPrime Total Genomic Labeling Module, Invitrogen) was added to each tube (total 50 μl) and mixed. Samples were incubated at 37°C for 2 h in a heating block in the dark. After the incubation, DNA was purified using an Invitrogen column provided in the labeling system and eluted in 55 μl of elution buffer. Labeling efficiency was determined using the MicroArray Measurement Module on the Nanodrop ND-1000 Spectrophotometer. The NanoDrop software facilitates the measurement of DNA concentration and dye labeling effectiveness. The NanoDrop ND-1000 Spectrophotometer measures the absorbance of the fluorescent dye, allowing detection at dye concentration as low as 0.2 pmol/ml. (http://www .nanodrop.com/Library/nd-1000-v3.7-users-manual-8 .5x11.pdf pg 30 for more details). An amount of 50 μl of labeled IP sample and 50 μl of labeled input samples were combined, and precipitated by the addition of 12 μl of NaAc (3M), 5 μl of Polyacrylamide (2.5 μg/ml) and 290 μl of absolute ethanol at −80°C for 10 min. DNA was pelleted by centrifugation, washed once with cold 75% ethanol, and resuspended in 37.5 μl of H_2O.

Hybridization

To the 37.5 μl of labeled samples were added 12.5 μl of Human Cot-1 DNA (1.0 mg/ml, Invitrogen), 12.5 μl of Agilent Blocking Agent (10×) and 62.5 μl of Agilent Hybridization Buffer (2x). 110μl of this hybridization mixture was applied to each Agilent yeast microarray (4 × 44k) http://www.genomics.agilent.com/CollectionSubpage .aspx?PageType = Product&SubPageType = ProductData &PageID = 1476) for hybridization for 24 h at 65°C as described in the Agilent ChIP on chip protocol.

Washing and scanning

After hybridization the microarrays were washed and scanned as described in the Agilent ChIP on chip protocol.

Feature extraction

The scanned image was analyzed by Agilent Feature extraction software. Red and green background subtracted signals were used for data analysis.

RESULTS

Detecting CPDs throughout the entire yeast genome

Yeast cells were irradiated with UV and then sampled either immediately or allowed a 2 h repair period. DNA purified from an unirradiated control (U), immediately after UV (0) and after UV with the 2-h repair period was sonicated to generate short fragments ranging from 200 to 800 bp and averaging 400 bp (input samples). Immunoprecipitation with the CPD antibody was carried out for unirradiated and UV irradiated samples (IP samples). We consistently detected over a 50-fold enrichment of DNA in the UV exposed samples compared with the unirradiated samples. We processed the IP and the input samples for microarray analysis employing the Agilent 4×44K yeast microarrays by labeling the IP sample with cy5 and the input sample with cy3. The ratio of the signals between the IP and the input samples for each probe on the microarray indicates the relative level of CPDs detected at the region the probe locates. Figure 1 shows a snapshot of CPD induction in part of chromosome 4 following a UV dose of 50 J/m^2. The data are the average of two independent experiments. The black line indicates the relative CPD level detected with the CPD antibody using the $\log_2$ ratio of the IP and the input sample signals, with the peaks representing high levels and the troughs low levels of CPDs. Error bars shown on the black line are 1 SD from the mean from the two individual experiments. It is evident that the induction of CPDs is heterogeneous along the genome.

Theoretical CPD distribution throughout the entire yeast genome

UV light, specifically at or near to 254 nm, is close to the maximum absorption wavelength of DNA. This UV radiation can generate many lesions, mainly at adjacent pyrimidine sites. Two adjacent pyrimidines in the same polynucleotide chain can absorb UV energy to form a four-membered ring structure, a CPD, resulting from saturation of the $C = C$ double bonds. CPDs form solely at adjacent pyrimidine sites, and their position is determined by the DNA sequence. The yield is influenced by the nucleotide composition of DNA and the quantitative ratio of CPD formation after UV irradiation at TT, TC, CT, CC sites is 68:16:13:3 as measured with plasmid DNA

(10) or human cells (11). Based on this ratio, we mathematically modeled the theoretical CPD distribution for the whole yeast genome from its sequence by taking account of the mean sheared average DNA fragment size of 400 bp.

A Perl script was written to generate a predicted binding level for each probe on the microarray based on the frequency of dipyrimidine sequences in the genomic region surrounding the ~60-nt region complementary to the probe sequence. At each complementary probe location the genomic region able to bind that probe was analyzed. This was calculated as the length of the mean sheared DNA fragment size up and downstream of the end and start of the complementary probe region, giving a sequence twice the length of the mean sheared DNA fragment size minus the probe size (Figure 2).

For each probe sequence region, a value was calculated for all dipyrimidines which were summed to assign a value to the probe, using the following Formula 1.

$$\text{Probe value} = \sum_{s=0}^{s=n} \frac{f - d_s}{f} \, p_s$$

Formula 1. Calculation of CPD probe values. s = dipyrimidine site, n = number of dipyrimidine sites, f = mean fragment length, d = distance of dipyrimidine site from probe, P = probability of a CPD occurring at the dipyrimidine site (TT/AA = 0.68, TC/GA = 0.16, CT/AG = 0.13, CC/GG = 0.03).
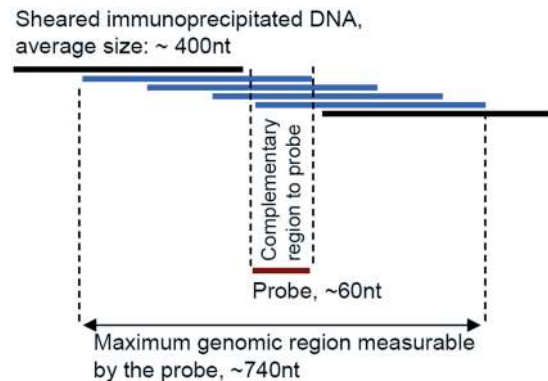
Figure 2. An outline showing the detectable genomic region for a probe (not to scale). All detectable fragments are in blue.
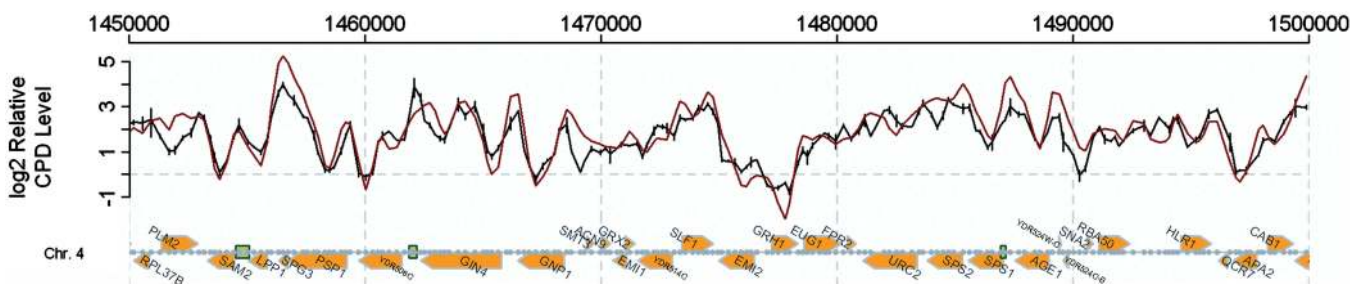
Figure 1. The CPD distribution in a part of Chromosome 4. Black: CPD level detected by the CPD antibody. Error bars shown on the black line are 1 SD from the mean from the two individual experiments. Red: theoretical CPD distribution. For the genome representations here and in the supplementary figures: yellow boxes show ORF positions (arrows indicate direction of transcription), green boxes are ARSs and blue boxes are centromeres and telomeres. Grey dots show probe positions.

Plotting the predicted CPD distribution from the sequence (red line) against the detected CPD values (black line) in part of the chromosome 4 (Figure 1) and for the entire genome (Supplementary Figure S1) show a remarkably good relationship. The Spearman rank correlation co-efficient (a non-parametric test) is 0.83 for the probes in Figure 1 and 0.77 for the entire genome, both with $P < 0.001$. Hence there is statistically significant relationship between the two sets of values.

Repair of CPDs in wild type and *rad4* cells

The comparison of the CPD levels immediately after UV versus 2 h repair in medium after UV should reflect the repair extent. We confirmed that these changes in signals actually reflect repair in two ways. First, whilst NER operates to remove CPDs from the nuclear genome, CPDs in mitochondrial DNA persist because NER does not operate in this organelle (12,13). The Agilent *S. cerevisiae* microarray includes hundreds of probes for detecting the mitochondrial genome. Therefore, the persistence of CPDs in mitochondrial DNA (Figure 3) serves as one quality control for interpreting the changes in the CPD levels seen with the nuclear probes. An example of the relative 2 h repair rate for part of chromosome 4 in repair competent cells is shown in Figure 4 (black line). Here the data are the average of two independent experiments. The peaks indicate fast repair and the troughs indicate slow repair. Repair is heterogeneous along the genome with a varied repair rate from region to region. Data for the whole genome are presented in Supplementary Figure S2.

To further verify that the change in CPDs detected at 2-h repair after UV is due to repair, CPDs were measured in a NER-deficient *rad4* mutant. This strain has a deletion of the yeast gene homologous to that which is defective in

Figure 3. Scatter plot of CPD levels before repair (CPD 0 h) versus 2 h repair (CPD 2 h). Red symbols: mitochondrial DNA (probes for all coding region in mitochondrial DNA where the GC content is closer to than in nuclear DNA); Grey symbols: nuclear DNA. Each data point is for a specific genomic probe.

human xeroderma pigmentosum sufferers belonging to complementation group C, and who are cancer-prone (1). In *S. cerevisiae* the *rad4* mutant is defective in both global and transcription-coupled NER (1,14). CPD repair was not detected, as shown by the red line in Figure 4 (the whole genome data are supplied in Supplementary Figure S2). These *rad4* data are the average of three independent experiments. Thus the changes in this ratio in the NER proficient cells are unequivocally due to NER. Consequently, this microarray approach can measure CPD induction and repair throughout the genome.

DISCUSSION

This combination of immunoprecipitation and microarray technology for examining the presence of DNA damage enables researchers to analyze repair events throughout an entire genome. Analyses of genome-wide DNA repair can be undertaken, alongside examination of the DNA damage-induced changes in chromatin that facilitate repair. For example, one can examine UV-induced changes in histone acetylations, other covalent histone modifications, the recruitment of specific enzymes such as histone acetyltranferases and histone deacetylases, the changes in nucleosome positions and the chromatin remodeling factors responsible for this. These events can be examined alongside the sequential recruitment of DNA repair enzymes. Such experiments are crucial to identify where in the genome the requirements differ for the chromatin modification enabling efficient NER (2). The approach should be applicable to examining other DNA damages provided either the antibodies or the tagged DNA damage recognition enzymes are available to immunoprecipitate those specific DNA damages, and provided that any of those damages that block PCR can be repaired to enable PCR. Those damages repairable by the PreCR kit can be seen on the following web site: http://www.neb.com/nebecomm/products/productM0309.asp. For damages not repairable by this kit (e.g. 8-oxo-7, 8-dihydro-2′adenosine), an alternative means of repair could be sought. The method should be applicable to studies with human cells via the available higher resolution human microarrays. Studies with human cells would employ $5–20 \, J/m^2$ at 260 nm, as these cells are more UV sensitive than is yeast; experiments are underway to optimize this approach with such cells. DNA samples prepared for this microarray-based approach can be readily processed for high throughput sequencing analysis if this is preferred, or if microarrays are unavailable for the organism of interest.

Finally, the technique has implications for monitoring the targets of existing and new anti-cancer chemotherapeutics that act through damaging DNA, or for genotoxicity testing. It will enable an estimation of the target sequences for DNA damage and whether these interactions persist in cells. A British Initial Patent application covering the technology was filed at the UK patent office on 28 June 2007, it entered the international PCT phase in 06/08 patent No. 0712584.2
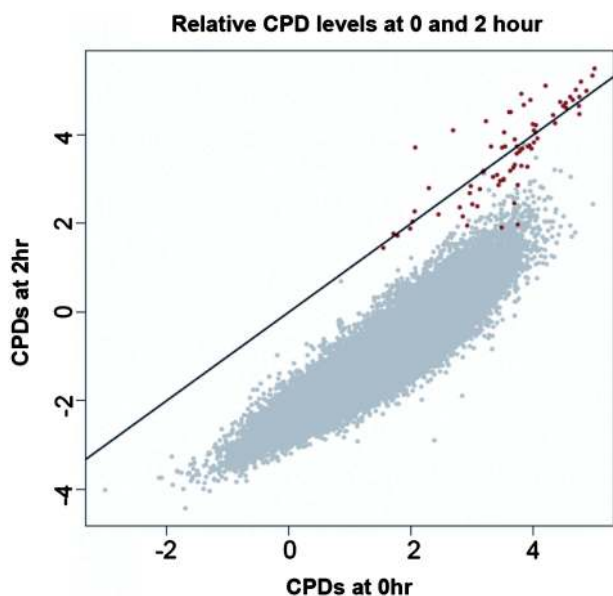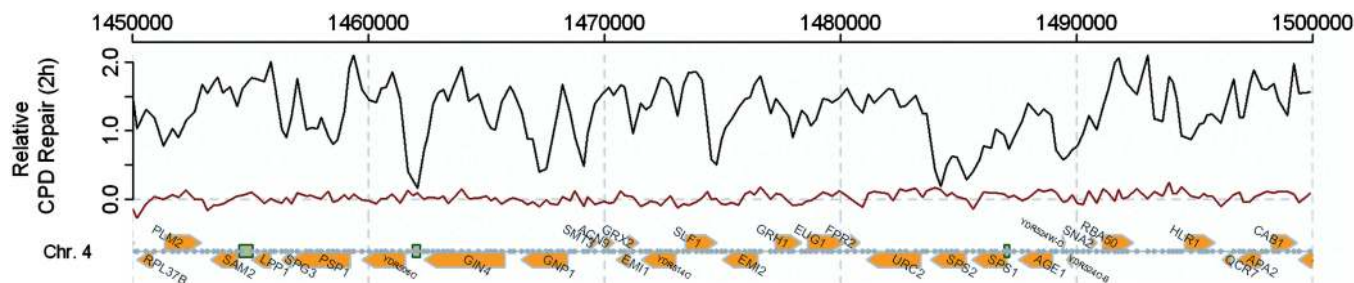
Figure 4. Relative CPD repair rate in a part of chromosome 4. Black: NER proficient cells; Red: NER deficient *rad4* cells. Nomenclature for the genome is as per Figure 1.

SUPPLEMENTARY DATA

Supplementary Data are available at NAR Online.

FUNDING

Conflict of interest statement. None declared.

REFERENCES

1. Friedberg,E., Walker,G.C., Siede,W., Wood,R.D., Schultz,R.A. and Ellenberger,T. (2005) *DNA Repair And Mutagenesis*, 2nd edn. ASM Press.
2. Waters,R., Teng,Y., Yu,Y., Yu,S. and Reed,S.H. (2009) Tilting at windmills? The nucleotide excision repair of chromosomal DNA. *DNA Repair*, **8**, 146–152.
3. Teng,Y., Yu,Y., Ferreiro,J.A. and Waters,R. (2005) Histone acetylation, chromatin remodelling, transcription and nucleotide excision repair in S. cerevisiae: studies with two model genes. *DNA Repair*, **4**, 870–883.
4. Verhage,R., Zeeman,A.M., de Groot,N., Gleig,F., Bang,D.D., van de Putte,P. and Brouwer,J. (1994) The RAD7 and RAD16 genes, which are essential for pyrimidine dimer removal from the silent mating type loci, are also required for repair of the nontranscribed strand of an active gene in Saccharomyces cerevisiae. *Mol. Cell Biol.*, **14**, 6135–6142.
5. Teng,Y., Li,S., Waters,R. and Reed,S.H. (1997) Excision repair at the level of the nucleotide in the Saccharomyces cerevisiae MFA2 gene: mapping of where enhanced repair in the transcribed strand begins or ends and identification of only a partial rad16 requisite for repairing upstream control sequences. *J. Mol. Biol.*, **267**, 324–337.
6. Spivak,G., Pfeifer,G.P. and Hanawalt,P. (2006) In vivo assays for transcription-coupled repair. *Methods Enzymol.*, **408**, 223–246.
7. Teng,Y., Yu,S., Reed,S.H. and Waters,R. (2009) Lux ex tenebris: nucleotide resolution DNA repair and nucleosome mapping. *Methods*, **48**, 23–34.
8. Mockler,T.C., Chan,S., Sundaresan,A., Chen,H., Jacobsen,S.E. and Ecker,J.R. (2005) Applications of DNA tiling arrays for whole-genome analysis. *Genomics*, **85**, 1–15.
9. Pokholok,D.K., Harbison,C.T., Levine,S., Cole,M., Hannett,N.M., Lee,T.I., Bell,G.W., Walker,K., Rolfe,P.A., Herbolsheimer,E. *et al.* (2005) Genome-wide map of nucleosome acetylation and methylation in yeast. *Cell*, **122**, 517–527.
10. Mitchell,D.L., Jen,J. and Cleaver,J.E. (1992) Sequence specificity of cyclobutane pyrimidine dimers in DNA treated with solar (ultraviolet B) radiation. *Nucleic Acids Res.*, **20**, 225–229.
11. Tornaletti,S., Rozek,D. and Pfeifer,G.P. (1993) The distribution of UV photoproducts along the human p53 gene and its relation to mutations in skin cancer. *Oncogene*, **8**, 2051–2057.
12. Waters,R. and Moustacchi,E. (1974) The fate of ultraviolet-induced pyrimidine dimers in the mitochondrial DNA of Saccharomyces cerevisiae following various post-irradiation cell treatments. *Biochim. Biophys. Acta*, **366**, 241–250.
13. Clayton,D.A., Doda,J.N. and Friedberg,E.C. (1974) The absence of a pyrimidine dimer repair mechanism in mammalian mitochondria. *Proc. Natl Acad. Sci. USA*, **71**, 2777–2781.
14. Prakash,L. (1977) Repair of pyrimidine dimers in radiation-sensitive mutants rad3, rad4, rad6 and rad9 of Saccharomyces cerevisiae. *Mutat. Res.*, **45**, 13–20.